Adiabatic sheath model for beam-driven blowout plasma channels

Yulong Liu, 1,2 Ming Zeng, 1,2,* Lars Reichwein, 3,4 and Alexander Pukhov 3

¹Institute of High Energy Physics, Chinese Academy of Sciences, Beijing 100049, China

²University of Chinese Academy of Sciences, Beijing 100049, China

³Institut für Theoretische Physik I, Heinrich-Heine-Universität Düsseldorf, 40225 Düsseldorf, Germany

⁴Peter Grünberg Institut (PGI-6), Forschungszentrum Jülich, 52425 Jülich, Germany

(Received 18 November 2024; accepted 14 April 2025; published 30 April 2025)

In plasma wakefield accelerators, the structure of the blowout sheath is vital for the blowout radius and the electromagnetic field distribution inside the blowout. Most previous theories assume artificial distribution functions for the sheath, which are either inaccurate or require prior knowledge of parameters. In this paper, we use an adiabatic sheath model based on force balancing to overcome these limitations. This model gives self-consistent forms of the sheath and pseudopotential distribution and estimates the balancing radius of the blowout channel better than previous models. Our findings not only enhance the understanding of sheath dynamics but also offer a self-consistent theoretical foundation for future studies on nonlinear phenomena in the blowout channel.

DOI: 10.1103/PhysRevResearch.7.023101

I. INTRODUCTION

Beam-driven plasma wakefield accelerators (PWFAs) have the capacity to accelerate particles to tens of GeV energies in meter-scale structures, making them competitive candidates for future high-energy accelerators that are used for next-generation particle colliders and x-ray free-electron lasers [1–7]. In a PWFA, when a high-current, relativistic electron beam, called the *drive beam*, interacts with an underdense plasma, plasma electrons are completely radially expelled while the ions remain immobile due to their much larger mass, forming an electron-free ion channel along the propagation axis. The physics of plasma response in this regime is strongly nonlinear, and the regime has been referred to as the blowout or bubble regime. In this regime, the acceleration (or deceleration) field is uniform and the focusing field is linear with regard to the radial offset from the axis [8–12].

On the boundary of the bubble, the expelled electrons form a narrow sheath, where the electron density and current profiles steepen with a large value and decay in a small thickness [13–15]. The sheath structure depends on the properties of the drive beam and is strongly correlated with the creation of the plasma blowout, the structure of wakefield inside the blowout, and the processes of particle injection into the wakefield [16–18].

Existing theories have used rectangular or exponential distributions to simplify the sheath shape [19–24]. Dalichaouch

Published by the American Physical Society under the terms of the Creative Commons Attribution 4.0 International license. Further distribution of this work must maintain attribution to the author(s) and the published article's title, journal citation, and DOI.

et al. [25] proposed a multisheath model, which employs two sheath layers to describe the wakefield more accurately. However, these models require the prior knowledge of the sheath thickness, which cannot be obtained self-consistently. Recently, Golovanov et al. [26] have developed a blowout theory from the energy conservation point of view. They have assumed a δ -function distribution for the blowout sheath and found the evolution function for the blowout channel radius r_{δ} as

$$A(r_{\delta})r_{\delta}\frac{d^2r_{\delta}}{d\xi^2} + B(r_{\delta})r_{\delta}^2 \left(\frac{dr_{\delta}}{d\xi}\right)^2 + Cr_{\delta}^2 = \Lambda, \qquad (1)$$

where $A=1+r_{\delta}^2/4$, $B=1/2+1/r_{\delta}^2$, and $C=\frac{1}{4}$. Here, $\xi=ct-z$ is the longitudinal comoving coordinate, c is the speed of light in vacuum, t is time, and z is the longitudinal coordinate. The drive term of the equation can be written as $\Lambda=2I/I_A$, where I is the instant current of the beam, $I_A=4\pi\epsilon_0 m_e c^3/e\approx 17$ kA is the Alfvén current, ϵ_0 is the vacuum permittivity, m_e is the electron rest mass, and e is the elementary charge [27–29]. If derivatives of r_{δ} are assumed to be zero, one can obtain the balancing radius of the channel based on the δ -sheath theory as

$$r_{\delta 0} = 2\sqrt{\Lambda}.\tag{2}$$

By contrast, the charge neutralization radius

$$r_n = \sqrt{2\Lambda} \tag{3}$$

has been widely accepted as the balancing radius from the electrostatic point of view [12,28,30].

In this paper, we develop a self-consistent model for the channel sheath using the adiabatic assumption [31]. The sheath equations are examined in two cases with the help of particle-in-cell (PIC) simulations. We demonstrate that our model provides a more accurate description of blowout

^{*}Contact author: zengming@ihep.ac.cn

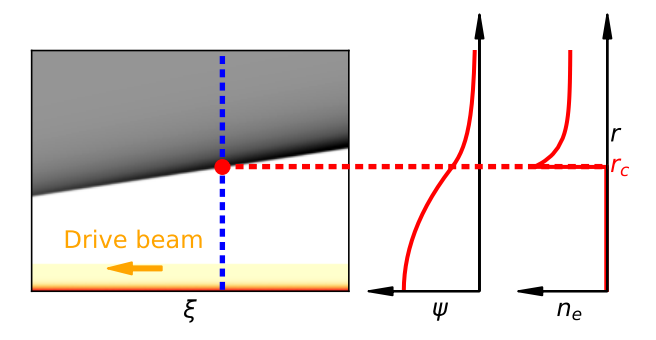


FIG. 1. Illustration of the adiabatic sheath model in this paper. The electron beam (orange, beam head is not shown), with a linear density $\Lambda(\xi)$, is moving to the left along the ξ axis and drives the plasma wakefield in the blowout regime. The plasma electrons (gray region) are completely evacuated in the channel with the radius $r_c(\xi)$, leaving an immobile ion column (white region). As Λ varies slowly with ξ in our assumption, the transverse electromagnetic balance is achieved everywhere. The right two subplots show the transverse distribution of the pseudopotential ψ and the electron density n_e at a certain ξ denoted by the blue dashed line.

channel balancing, as its predicted channel radius falls between the electrostatic neutralization radius and that predicted by the δ -sheath theory.

Throughout the paper, we adopt the plasma normalization units, in which charge is normalized to e, mass to m_e , velocity to c, density to plasma density n_p , time to ω_p^{-1} , length to c/ω_p , electric field to $m_e c \omega_p/e$, magnetic field to $m_e \omega_p/e$, electrostatic potential to $m_e c^2/e$, and vector potential to $m_e c/e$, where $\omega_p = \sqrt{e^2 n_p/\epsilon_0 m_e}$ is the plasma frequency.

II. MODEL DESCRIPTION

We consider a highly relativistic drive electron beam with density $n_b(\xi, r)$ that expels the plasma electrons to form an ion channel with a radius $r_c(\xi)$, where r is the radial coordinate, and cylindrical symmetry is assumed. We assume that the drive beam is narrower than the channel, so that there is no drive charge outside the channel, or $n_b = 0$ for $r > r_c$. Under these assumptions, the drive term can also be written as $\Lambda(\xi) = \int_0^\infty n_b r dr$, which has the physical meaning of the (normalized) linear density of the drive beam.

Furthermore, we assume the radius of the ion channel changes adiabatically, which means $(dr_c/r_c)/d\xi \ll 1$, $(d\Lambda/\Lambda)/d\xi \ll 1$, and $\partial_{\xi} \ll \partial_r$ for all field variables, as illustrated in Fig. 1. Under the cylindrical symmetry and the quasistatic approximation [32,33], the pseudopotential of the wakefield obeys the following Poisson-like equation [12,34]:

$$-\frac{1}{r}\frac{\partial}{\partial r}\left(r\frac{\partial}{\partial r}\psi\right) = S,\tag{4}$$

where $\psi = \varphi - A_z$ is the pseudopotential, φ is the electrostatic potential, A_z is the longitudinal component of the vector potential,

$$S = \rho - J_z = 1 - n_e (1 - v_z) \tag{5}$$

is the source term, ρ is the charge density, J_z is the longitudinal component of the current density, n_e is the plasma electron

density, and v_z is the longitudinal velocity of the plasma electrons. Because $n_e = 0$ for $r < r_c$, we can write the form of the pseudopotential inside the blowout

$$|\psi|_{r < r_c} = \psi_c + \frac{r_c^2}{4} - \frac{r^2}{4},$$
 (6)

where

$$\psi_c = \psi|_{r=r_c} > 0 \tag{7}$$

is to be determined. It can be derived that $\psi_c=0$ with the δ -function distribution, i.e., $S=1-H(r-r_c)-r_c\delta(r-r_c)/2$, where H is the Heaviside step function, and δ is the Dirac delta function. However, in this paper, S is finite everywhere, so that ψ_c is nonzero, and $\partial \psi/\partial r$ is continuous everywhere because of Eq. (4), which means

$$\left. \frac{\partial}{\partial r} \psi \right|_{r=r_c} = -\frac{r_c}{2}.\tag{8}$$

The other boundary condition is

$$\lim_{\tau \to \infty} \psi = 0, \tag{9}$$

which is a natural requirement that the plasma disturbance is local.

For a plasma electron which is at rest before the drive beam arrives, there is a constant of motion [33]

$$\gamma - v_z \gamma - \psi = 1, \tag{10}$$

where $\gamma = 1/\sqrt{1 - v_z^2 - v_r^2}$ is the Lorentz factor, and v_z and v_r are the longitudinal and radial components of the velocity of the electron, respectively. This equation can be solved under the adiabatic assumption, which means $v_r \approx 0$, as

$$v_z = \frac{2}{1 + (1 + \psi)^2} - 1. \tag{11}$$

Based on the adiabatic assumption, the transverse electromagnetic field can be written using Gauss's law and Stokes' theorem

$$E_r = \frac{r}{2} - \frac{\Lambda}{r} - \frac{1}{r} \int_0^r n_e(r')r'dr',$$
 (12)

$$B_{\theta} = -\frac{\Lambda}{r} - \frac{1}{r} \int_{0}^{r} n_{e}(r')v_{z}(r')r'dr'.$$
 (13)

The transverse force $F_r = -E_r + v_z B_\theta$ should be balanced for $r > r_c$, which means

$$0 = rF_r = -\frac{r^2}{2} + (1 - v_z)\Lambda + \int_0^r n_e(r')r'dr'$$
$$-v_z \int_0^r n_e(r')v_z(r')r'dr'. \tag{14}$$

The channel radius is determined by letting $r = r_c$ in Eq. (14), as

$$r_c = \sqrt{2(1 - v_{zc})\Lambda} = 2\sqrt{\frac{\Lambda}{1 + \frac{1}{(1 + \psi_c)^2}}},$$
 (15)

where

$$v_{zc} = v_z|_{r=r_c} = \frac{2}{1 + (1 + \psi_c)^2} - 1.$$
 (16)

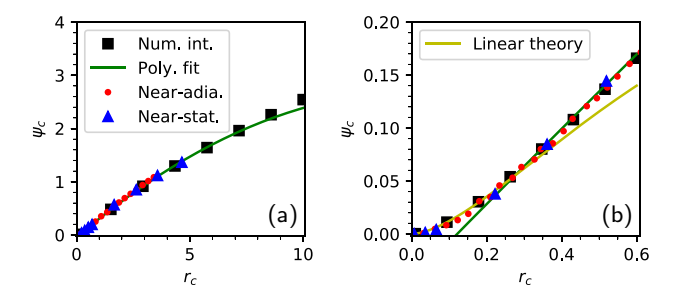


FIG. 2. Comparison of ψ_c vs r_c obtained by the numerical integral of Eqs. (4), (11), and (14) using the boundary conditions Eqs. (8) and (9) (black squares), by the polynomial fit Eq. (17) (green line), by the linear theory Eq. (22) (yellow line), by PIC simulations in near-adiabatic cases (red dots) and in near-stationary cases (blue triangles). Both (a) large and (b) small scales of r_c are plotted to show the different asymptotic behavior of ψ_c at the two ends.

We see that r_c reduces to r_n if $\psi_c = 0$ and to $r_{\delta 0}$ if $\psi_c \to \infty$. Then we know $r_n < r_c < r_{\delta 0}$ if ψ_c is nonzero and finite because r_c monotonically increases with ψ_c .

III. MODEL SOLUTION

The sheath model defined by Eqs. (4), (11), and (14) is solvable using the left boundary condition Eq. (8) and the right boundary condition Eq. (9). We use the shooting method to numerically solve the equations. In other words, the numerical integral is performed from $r = r_c$ to a sufficiently large value of r, while ψ_c is predicted and corrected in iterations, so that Eq. (9) is satisfied to a certain accuracy. Practically, there is a critical value of ψ_c for each r_c , which prevents divergence at large r. The Python script for the numerical solution is in the Supplemental Material [35] and is maintained on GitHub [36]. The numerical solution of ψ_c with different r_c is shown in Fig. 2. The polynomial fit

$$\psi_c \approx -0.012r_c^2 + 0.363r_c - 0.044 \tag{17}$$

is a good estimate for $r_c \lesssim 8$, as shown in Fig. 2(a).

After ψ_c is obtained, the electron density at the sheath boundary can be predicted. By taking the derivative of Eq. (14), we obtain

$$n_e r \left(1 - v_z^2\right) = r + \Lambda \frac{\partial v_z}{\partial r} + \frac{\partial v_z}{\partial r} \int_0^r n_e(r') v_z(r') r' dr'. \quad (18)$$

At $r = r_c$, the integral is zero, the derivative of v_z can be determined by Eqs. (8) and (11), and Λ can be written as the function of r_c and ψ_c according to Eq. (15). As a result,

$$n_e|_{r=r_c} = \frac{r_c^2}{8} \left(\frac{1}{\psi_*} + \frac{1}{\psi_*^3}\right) + \frac{1}{4} \left(\psi_* + \frac{1}{\psi_*}\right)^2,$$
 (19)

where $\psi_* = 1 + \psi_c$.

Next, we study the behavior of ψ and ψ_c in the limit $\psi_c \ll 1$. This also means $r_c \ll 1$, $\Lambda \ll 1$, and $\psi \ll 1$. By expanding Eqs. (11) and (18) and keeping only the first-order terms of ψ , we have $v_z \approx -\psi$ and $n_e \approx 1$. Thus, the linear form of Eq. (4) is obtained

$$\frac{\partial^2}{\partial r^2}\psi + \frac{1}{r}\frac{\partial}{\partial r}\psi - \psi = 0. \tag{20}$$

The solution satisfying the right boundary condition Eq. (9) is $\psi = R(r_c)K_0(r)$, where $R(r_c)$ is a constant of r to be determined, and $K_0(r)$ is the modified Bessel function of the second kind of order zero [37]. By also considering the left boundary condition Eq. (8), we may get the expression of $R(r_c)$ to the lowest order of r_c and find

$$\psi|_{r>r_c} = \frac{r_c^2}{2} K_0(r). \tag{21}$$

Thus,

$$\psi_c = \frac{r_c^2}{2} K_0(r_c), \tag{22}$$

or $\psi_c \approx -\frac{r_c^2}{2}(\ln\frac{r_c}{2} + 0.577...)$, where the second summand is the Euler-Mascheroni constant. We can see in Fig. 2(b) that Eq. (22) is satisfactory with the numerical results for $r_c \lesssim 0.28$, while Eq. (17) is better for $r_c \gtrsim 0.28$.

IV. COMPARISON WITH SIMULATIONS

Once ψ_c is determined, the one-to-one mapping between Λ and r_c can be obtained according to Eq. (15). For comparison, PIC simulations have been performed using the quasistatic code QuickPIC [38,39]. In the simulations, we consider a 5 GeV drive electron beam, transversely positioned at x=y=0 (i.e., the center of the simulation domain). It has a sufficiently small transverse size, while its longitudinal size is the same as the entire simulation domain. Two sets of simulations with different drive beam current profiles have been conducted. One is called the near-adiabatic profile, where Λ increases linearly with a sufficiently small slope. The other is called the near-stationary profile, where Λ increases from 0 to a plateau, and the increasing profile and length are designed so that the oscillation of the channel radius in the plateau is not severe.

In the near-adiabatic simulations, we have chosen the maximum $\Lambda_{\rm max}=4$ for the large r_c scale shown in Figs. 2(a) and 3(a) and $\Lambda_{\rm max}=0.4$ for the small r_c scale shown in Fig. 2(b). The simulation domain has a size of 200 in the ξ direction, which is the propagation direction, and 40 (10) in the x and y directions for the $\Lambda_{\rm max}=4$ (0.4) case. The numbers of cells are 2048, 1024, and 1024, respectively. The near-adiabatic simulation results for ψ_c vs r_c are shown in Fig. 2, which are in good agreement with our model.

In the near-stationary simulations, Λ increases from 0 to the plateau value Λ_0 within $0 \leqslant \xi \leqslant 25$ and keeps the plateau value in the remaining of the simulation domain, as shown in Fig. 3(c). Cubic splines have been designed to smooth the transitions near $\xi=0$ and 25. Here, the simulation domain has a longitudinal size of 48, while the transverse size is adjusted in accordance with Λ_0 , such that $\psi \to 0$ at the simulation boundary is guaranteed $(\partial \psi/\partial r \approx 0$ at the boundary), and the transverse resolution is adequate to resolve the sheath. Again, the number of cells is chosen to be $2048 \times 1024 \times 1024$. Here, Λ_0 has been scanned from 2.5×10^{-5} to 6.25 in the simulations. The results of ψ_c vs r_c are shown in Fig. 2, which are also in good agreement with our model.

Plasma density slices at y = 0 for two of the above-mentioned simulations are shown in Figs. 3(b) and 3(d). We compare the simulations with $r_{\delta 0}$ obtained by Eq. (2), r_n

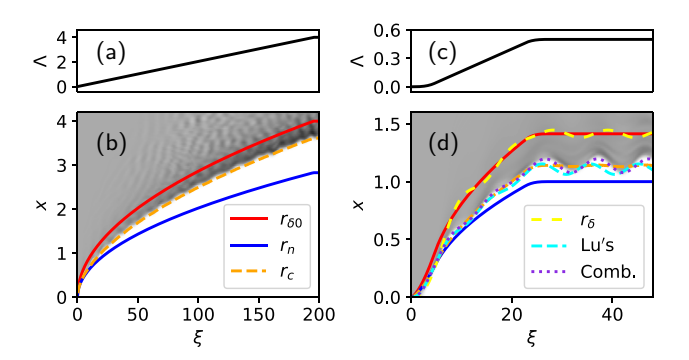


FIG. 3. The distribution of Λ and slice plots of plasma electron density at y=0 (gray) in simulations for (a) and (b) a near-adiabatic case and (c) and (d) a near-stationary case. The numerical solution of the balancing radius based on the δ -sheath theory r_{δ} (yellow dashed line) and its balance $r_{\delta 0}$ (red line), the neutralization radius r_n (blue line), the solution based on our theory r_c (orange dashed line), the numerical solution based on Lu's model with $\beta=1/r_c+0.1$ (cyan dashed line), and the combined model with β in Lu's model replaced by Eq. (23) (violet dotted line) are plotted for the comparison.

obtained by Eq. (3), and r_c obtained by Eq. (15). We see that the channel radius in simulations best matches with r_c , while r_n is an underestimate and $r_{\delta 0}$ is an overestimate.

V. COMBINED MODEL FOR THE OSCILLATION OF THE CHANNEL RADIUS

The channel radius slightly oscillates around r_c in the near-stationary case because of the imperfect balancing, as shown in Fig. 3(d). This oscillation be numerically behavior can solved using Lu's model [12,19], which is similar to Eq. (1), but the parameters are $A = 1 + [\frac{1}{4} + \beta/2 + (r_c/8)(d\beta/dr_c)]r_c^2$, $B = \frac{1}{2} + (\frac{3}{4})\beta + (3r_c/4)(d\beta/dr_c) + (r_c^2/8)(d^2\beta/dr_c^2),$ and $C = [1 + 1/(1 + \beta r_c^2/4)^2]/4$. The variable β needs prior knowledge to the sheath thickness and was recommended to be $\beta = 1/r_c + 0.1$. Although Lu's model is in good agreement with the simulation in the short drive cases (the drive beam is shorter than or comparable with the plasma wavelength), it has some slight error in the long drive cases, as shown in Fig. 3(d).

To improve Lu's model, we replace β by

$$\beta = \frac{4\psi_c}{r_c^2},\tag{23}$$

where ψ_c is expressed in a piecewise manner by Eq. (22) for $r_c < 0.28$ and by Eq. (17) for $r_c > 0.28$, and call it the *combined model*. The combined model has been applied to the near-stationary cases, with one example shown as the violet dotted line in Fig. 3(d). To quantitatively compare the results from the three models with those from the simulation, we calculate the average radius in the plateau of Λ distribution. Compared with the simulation result, our combined model only exhibits a 0.55% difference, while r_{δ} has a 24.28% difference, and Lu's model has a -2.11% difference. Moreover, we have observed that the oscillation frequency of the channel radius in Lu's model is slightly larger than the actual frequency. It should be noted that, in the near-adiabatic case, as shown

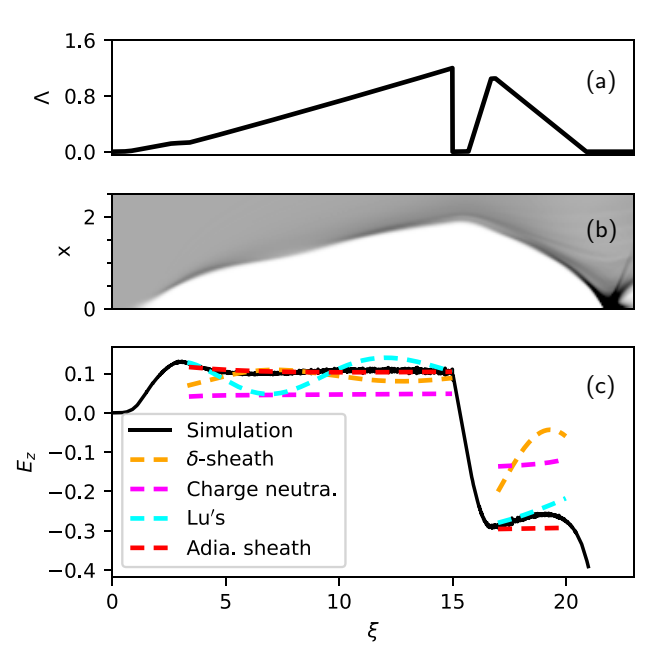


FIG. 4. The current profile design of a plasma wakefield accelerator with the transformer ratio of 3. (a) The distribution of Λ for both the driving ($0 \le \xi \le 15$) and trailing ($15.5 \le \xi \le 22$) beams. The profile is designed so that the major part of the beam witnesses constant deceleration (acceleration) field for the driving (trailing) beam according to our adiabatic sheath model, and cubic splines are used between the transitions to avoid abrupt changes. (b) The slice plot of the plasma electron density at y=0. (c) The comparison of the on-axis longitudinal electric field E_z from the simulation (black solid line) and based on the models: δ -sheath theory (orange dashed line), charge neutralization model (magenta dashed line), Lu's model with $\beta=1/r_c+0.1$ (cyan dashed line), and the adiabatic sheath model (red dashed line).

in Fig. 3(b), we do not show the curves of r_{δ} , Lu's model, and the combined model because the radii from Lu's model and the combined model are both approximately equal to r_c , and the curve of r_{δ} almost perfectly overlaps with that of $r_{\delta 0}$.

VI. APPLICATION IN HIGH TRANSFORMER RATIO ACCELERATION

We further show a practical application of the adiabatic sheath model in achieving high transformer ratio acceleration [40,41]. The longitudinal electric field inside the blowout is given by $E_z = d\psi_a/d\xi$, where $\psi_a = \psi|_{r=0}$ is the pseudopotential on axis and can be determined according to Eqs. (6), (15), (17), and (22). In most cases, $r_c > 0.28$, and it can be derived that the condition for achieving a constant E_z is

$$\Lambda \approx 1.05(U - 0.37)^{2} \left\{ 1 + \frac{1}{[3.73 - 0.05(U - 7.82)^{2}]^{2}} \right\}, \tag{24}$$

where

$$U = \sqrt{E_z \xi + C}. (25)$$

If the initial conditions given at $\xi = \xi_0$ are $r_c(\xi_0) = r_{c0}$ and $E_z(\xi_0) = E_{z0}$, the parameter C should be

$$C = 0.238r_{c0}^2 + 0.362r_{c0} + 0.14 - E_{z0}\xi_0$$
 (26)

to ensure that E_z remains the constant E_{z0} for $\xi > \xi_0$. We have applied this condition to design a profile of Λ shown in Fig. 4(a) and performed such a simulation shown in Fig. 4(b). The profile consists of two designed curves within $3.3 < \xi <$ 15 and 16.7 < ξ < 22 based on Eqs. (24) to (26) and cubic splines within $0 < \xi < 3.3$ and $15.5 < \xi < 16.7$ to smooth the transitions. In this case, the transformer ratio, defined as the acceleration field of the trailing beam divided by the deceleration field of the driving beam, is ~ 3 , and E_z from our adiabatic sheath model agrees best among the models with the simulation results in the deceleration phase 3.3 < ξ < 15, as shown in Fig. 4(c). We see that E_7 is almost a constant of 0.1 in this phase, which proves the validity of our design. Note that the design is not so satisfactory in the acceleration phase $16.7 < \xi < 22$ because the sheath has gained strong retraction momentum during the profile gap $15 < \xi < 15.5$, and the near-adiabatic status is difficult to be recovered. Nevertheless, the E_z within $16.7 < \xi < 22$ from the simulation has an average value of ~ -0.3 , which best agrees with our model among all the above-mentioned models.

VII. CONCLUSIONS

In conclusion, we have introduced a self-consistent model for the sheath structure of the blowout plasma channel driven by an electron beam based on the adiabatic assumption. The model consists of the equations for the pseudopotential Eq. (4), the longitudinal velocity of the sheath electrons Eq. (11), and the transverse force balancing condition Eq. (14), which is solvable with the boundary conditions Eqs. (8) and (9). An analytical solution is obtained in the small-blowout limit as Eq. (21), and a general solution is retrieved numerically by the shooting method. The PIC simulations show that the radius obtained by Eq. (15) is a better estimate of the channel balancing radius than that from previous neutralization or δ -sheath models.

It should be noted that the accuracy of our model is limited in short drive beam cases. Nevertheless, our model is very suitable for long drive beams. Especially by combining our model with Lu's model, we have obtained the most correct description of the oscillation of the channel radius. Furthermore, the ion motion may have to be considered for such long drive beam cases [42,43], unless the plasma background consists of heavy ions, which is to be addressed in a future work. The better understanding of the pseudopotential at the sheath boundary and inside the blowout for long drive cases is crucial for high transformer ratio and future high-energy PWFA studies [5,40,41].

ACKNOWLEDGMENTS

This paper is supported by the Strategic Priority Research Program of the Chinese Academy of Sciences (Grant No. XDB0530000), the National Natural Science Foundation of China (Grant No. 12475159), and the BMBF Project No. 05P24PF2 (Germany).

DATA AVAILABILITY

No data were created or analyzed in this study.

- [1] P. Chen, J. M. Dawson, R. W. Huff, and T. Katsouleas, Acceleration of electrons by the interaction of a bunched electron beam with a plasma, Phys. Rev. Lett. **55**, 1537(E) (1985).
- [2] I. Blumenfeld, C. E. Clayton, F.-J. Decker, M. J. Hogan, C. Huang, R. Ischebeck, R. Iverson, C. Joshi, T. Katsouleas, N. Kirby *et al.*, Energy doubling of 42 GeV electrons in a metrescale plasma wakefield accelerator, Nature (London) 445, 741 (2007).
- [3] C. Adolphsen et al., in European Strategy for Particle Physics— Accelerator R&D Roadmap, edited by N. Mounet (CERN, Geneva, 2022).
- [4] B. Foster, R. D'Arcy, and C. A. Lindstrøm, A hybrid, asymmetric, linear Higgs factory based on plasma-wakefield and radio-frequency acceleration, New J. Phys. 25, 093037 (2023).
- [5] J. Gao, CEPC technical design report: Accelerator, Radiat. Detect. Technol. Methods 8, 1 (2024).
- [6] W. Wang, K. Feng, L. Ke, C. Yu, Y. Xu, R. Qi, Y. Chen, Z. Qin, Z. Zhang, M. Fang *et al.*, Free-electron lasing at 27 nanometres based on a laser wakefield accelerator, Nature (London) 595, 516 (2021).
- [7] R. Pompili *et al.*, Free-electron lasing with compact beamdriven plasma wakefield accelerator, Nature (London) 605, 659 (2022).

- [8] T. Katsouleas, Physical mechanisms in the plasma wake-field accelerator, Phys. Rev. A 33, 2056 (1986).
- [9] J. J. Su, T. Katsouleas, J. M. Dawson, P. Chen, M. Jones, and R. Keinigs, Stability of the driving bunch in the plasma wakefield accelerator, IEEE Trans. Plasma Sci. 15, 192 (1987).
- [10] J. B. Rosenzweig, B. Breizman, T. Katsouleas, and J. J. Su, Acceleration and focusing of electrons in two-dimensional nonlinear plasma wake fields, Phys. Rev. A 44, R6189 (1991).
- [11] N. Barov and J. B. Rosenzweig, Propagation of short electron pulses in underdense plasmas, Phys. Rev. E **49**, 4407 (1994).
- [12] W. Lu, C. Huang, M. Zhou, M. Tzoufras, F. S. Tsung, W. B. Mori, and T. Katsouleas, A nonlinear theory for multidimensional relativistic plasma wave wakefields, Phys. Plasmas 13, 056709 (2006).
- [13] J. B. Rosenzweig, Nonlinear plasma dynamics in the plasma wake-field accelerator, Phys. Rev. Lett. 58, 555 (1987).
- [14] J. B. Rosenzweig, N. Barov, M. C. Thompson, and R. B. Yoder, Energy loss of a high charge bunched electron beam in plasma: Simulations, scaling, and accelerating wakefields, Phys. Rev. ST Accel. Beams 7, 061302 (2004).
- [15] I. Kostyukov, A. Pukhov, and S. Kiselev, Phenomenological theory of laser-plasma interaction in bubble regime, Phys. Plasmas 11, 5256 (2004).

- [16] M. Tzoufras, W. Lu, F. S. Tsung, C. Huang, W. B. Mori, T. Katsouleas, J. Vieira, R. A. Fonseca, and L. O. Silva, Beam loading in the nonlinear regime of plasma-based acceleration, Phys. Rev. Lett. 101, 145002 (2008).
- [17] I. Kostyukov, E. Nerush, A. Pukhov, and V. Seredov, Electron self-injection in multidimensional relativistic-plasma wake fields, Phys. Rev. Lett. 103, 175003 (2009).
- [18] A. A. Golovanov, I. Y. Kostyukov, J. Thomas, and A. Pukhov, Beam loading in the bubble regime in plasmas with hollow channels, Phys. Plasmas **23**, 093114 (2016).
- [19] W. Lu, C. Huang, M. Zhou, W. B. Mori, and T. Katsouleas, Non-linear theory for relativistic plasma wakefields in the blowout regime, Phys. Rev. Lett. **96**, 165002 (2006).
- [20] S. A. Yi, V. Khudik, C. Siemon, and G. Shvets, Analytic model of electromagnetic fields around a plasma bubble in the blow-out regime, Phys. Plasmas 20, 013108 (2013).
- [21] J. Thomas, I. Y. Kostyukov, J. Pronold, A. Golovanov, and A. Pukhov, Non-linear theory of a cavitated plasma wake in a plasma channel for special applications and control, Phys. Plasmas 23, 053108 (2016).
- [22] A. Golovanov, I. Kostyukov, A. Pukhov, and J. Thomas, Generalised model of a sheath of a plasma bubble excited by a short laser pulse or by a relativistic electron bunch in transversely inhomogeneous plasma, Quantum Electron. 46, 295 (2016).
- [23] A. A. Golovanov, I. Y. Kostyukov, J. Thomas, and A. Pukhov, Analytic model for electromagnetic fields in the bubble regime of plasma wakefield in non-uniform plasmas, Phys. Plasmas 24, 103104 (2017).
- [24] A. A. Golovanov, I. Y. Kostyukov, L. Reichwein, J. Thomas, and A. Pukhov, Excitation of strongly nonlinear plasma wakefield by electron bunches, Plasma Phys. Control. Fusion 63, 085004 (2021).
- [25] T. N. Dalichaouch, X. L. Xu, A. Tableman, F. Li, F. S. Tsung, and W. B. Mori, A multi-sheath model for highly nonlinear plasma wakefields, Phys. Plasmas **28**, 063103 (2021).
- [26] A. Golovanov, I. Y. Kostyukov, A. Pukhov, and V. Malka, Energy-conserving theory of the blowout regime of plasma wakefield, Phys. Rev. Lett. 130, 105001 (2023).
- [27] D. H. Whittum, A. M. Sessler, and V. K. Neil, Transverse resistive wall instability in the two-beam accelerator, Phys. Rev. A 43, 294 (1991).
- [28] C. Huang, W. Lu, M. Zhou, C. E. Clayton, C. Joshi, W. B. Mori, P. Muggli, S. Deng, E. Oz, T. Katsouleas *et al.*, Hosing instability in the blow-out regime for plasma-wakefield acceleration, Phys. Rev. Lett. **99**, 255001 (2007).
- [29] A. Martinez de la Ossa, T. J. Mehrling, L. Schaper, M. J. V. Streeter, and J. Osterhoff, Wakefield-induced ionization

- injection in beam-driven plasma accelerators, Phys. Plasmas 22, 093107 (2015).
- [30] A. A. Geraci and D. H. Whittum, Transverse dynamics of a relativistic electron beam in an underdense plasma channel, Phys. Plasmas 7, 3431 (2000).
- [31] D. H. Whittum, Nonlinear, relativistic return current sheath for an ionfocused beam, Phys. Fluids B 4, 476 (1992).
- [32] D. H. Whittum, Transverse two-stream instability of a beam with a Bennett profile, Phys. Plasmas 4, 1154 (1997).
- [33] P. Mora and T. M. Antonsen, Jr., Kinetic modeling of intense, short laser pulses propagating in tenuous plasmas, Phys. Plasmas 4, 217 (1997).
- [34] D. H. Whittum, W. M. Sharp, S. S. Yu, M. Lampe, and G. Joyce, Electron-hose instability in the ion-focused regime, *Phys. Rev. Lett.* **67**, 991 (1991).
- [35] See Supplemental Material at http://link.aps.org/supplemental/10.1103/PhysRevResearch.7.023101 for a code that numerically solves the adiabatic sheath model Eqs. (4), (8), (9), (11), and (14).
- [36] M. Zeng, https://github.com/mingzeng8/adiabatic_sheath_solver, the Git repository for the numerical solver of the adiabatic sheath model.
- [37] A. Jeffrey and H.-H. Dai, Handbook of Mathematical Formulas and Integrals, 4th ed. (Academic Press, Oxford, 2008).
- [38] C. Huang, V. K. Decyk, C. Ren, M. Zhou, W. Lu, W. B. Mori, J. H. Cooley, T. M. Antonsen, and T. C. Katsouleas, QuickPIC: A highly efficient particle-in-cell code for modeling wakefield acceleration in plasmas, J. Comput. Phys. 217, 658 (2006).
- [39] W. An, V. K. Decyk, W. B. Mori, and T. M. Antonsen, An improved iteration loop for the three dimensional quasi-static particle-in-cell algorithm: QuickPIC, J. Comput. Phys. 250, 165 (2013).
- [40] W. Lu, W. An, C. Huang, C. Joshi, W. Mori, M. Hogan, T. Raubenheimer, and A. Seryi, High transformer ratio PWFA for application on XFELs, in *Proceedings of Particle Accelerator Conference (PAC 09)* (Proceedings of PAC09, Vancouver, BC, Canada, 2010), p. WE6RFP098.
- [41] G. Loisch *et al.*, Observation of high transformer ratio plasma wakefield acceleration, Phys. Rev. Lett. **121**, 064801 (2018).
- [42] W. An, W. Lu, C. Huang, X. Xu, M. J. Hogan, C. Joshi, and W. B. Mori, Ion motion induced emittance growth of matched electron beams in plasma wakefields, Phys. Rev. Lett. 118, 244801 (2017).
- [43] C. Benedetti, C. B. Schroeder, E. Esarey, and W. P. Leemans, Emittance preservation in plasma-based accelerators with ion motion, Phys. Rev. Accel. Beams 20, 111301 (2017).